

Advancements in Quark-Gluon Measurement Using a Computational Approach

Kamil khan^{*1}, Muhammad Shershah¹, Muhammad Bilal¹, Nehad Ali¹, Wiqar Ahmad¹, Muhammad Arsalan¹, Tauseef Ahmad¹, Adnan Khan¹, Haider Ali Khan¹, Sardar Nabi¹, Jaweria Taj²

¹Department of Physics, Government Post Graduate College (506620) Mardan, Mardan23200, Pakistan

²Department of Physics, Government Post Graduate College for Women Mardan, Mardan23200, Pakistan

To cite this article:

Kamil khan, Muhammad Shershah, Muhammad Bilal, Nehad Ali, Wiqar Ahmad, Muhammad Arsalan, Tauseef Ahmad, Adnan Khan, Sardar nabi, Haider ali khan, Jaweria Taj. (2023). Advancements in Quark-Gluon Measurement Using a Computational Approach. Journal of Xi'an Shiyou University, *Volume*(19), Page Range. DOI Link

Abstract: This comprehensive study aims to address a fundamental inquiry: how can we attain a precise measurement of the gluon Parton Distribution Function (PDF) to enhance our comprehension of the intricate quark-gluon composition within nucleons? Employing a dual methodology that integrates Quantum Chromodynamics (QCD) and high-energy particle collisions, our research leverages computational tools and experimental techniques, with a specific focus on probing protons and neutrons. Through scattering experiments and advanced detectors, we delve into the intricate structure of nucleons.

The investigation encompasses a synergy of theoretical frameworks, notably utilizing QCD equations and the Momentum Sum Rule to scrutinize Parton Distribution Functions at distinct momentum fractions and energy scales. Our primary objective is to achieve an unparalleled precision in measuring the gluon PDF, a paramount undertaking crucial for unraveling the complexities associated with the strong force and internal dynamics of nucleons.

Incorporating theoretical plots and equations, our study vividly illustrates the hypothetical behaviors of gluon distribution, quark distribution, and splitting functions. These representations contribute significantly to a profound understanding of fundamental particles, shedding light on the underlying dynamics and interactions that govern their behavior. By combining computational simulations with real-world experimental data, this research offers a holistic approach, advancing our knowledge of the intricate interplay between quarks and gluons within nucleons, ultimately contributing to the broader understanding of the fabric of matter.

Keywords: Quantum Chromo Dynamics (QCD), Parton Distribution Functions (PDFs), DGLAP Evolution Equation, Quarks and Gluons, Monte Carlo Simulations, Uncertainties in α_s (MZ)

1. Introduction

Our exploration into the quark-gluon structure of nucleons is guided by an intricate methodology that seamlessly intertwines computational and experimental techniques. This approach seeks to unravel the elusive distribution of quarks and gluons nestled within nucleons, providing a comprehensive understanding of their internal mechanisms.

Key to our investigative technique is the utilization of experimental procedures, which involve high-energy particle collisions. Accelerators, which impart significant energy to particles in the form of hadrons or leptons, serve as our tools. By directing these high-energy projectiles toward nucleon targets, we can directly probe the interior structure of nucleons [1, 2].

The experiments, in the form of scattering experiments, entail launching high-energy particles at nucleon targets and meticulously measuring the paths and energies of the scattered particles. It is through the analysis of these dispersed particles that we deduce intricate details about the internal components

of the nucleon.

To meticulously collect and scrutinize the particles resulting from collisions, we employ sophisticated particle detectors—calorimeters, spectrometers, and tracking detectors. These detectors allow us to monitor the routes and energy of departing particles, a crucial aspect for unraveling the quark-gluon structure.

In tandem with experimental data, computational techniques play a pivotal role in our research. Theoretical models and numerical simulations empower us to analyze and comprehend the intricate data gleaned from experiments. One such theoretical framework central to our study is Quantum Chromodynamics (QCD), which eloquently describes the strong force governing quark interactions. [3]

A critical aspect of our computational techniques involves tests for scattering. These tests, rooted in Quantum Chromodynamics (QCD), play a crucial role in elucidating the strong force dynamics and the behavior of quarks and gluons.

Through simulations based on QCD equations, we can anticipate and model the interactions within nucleons, revealing their quark and gluon distributions.

Monte Carlo simulations, a sophisticated technique employed in our study, allow us to model complex particle interactions and hadronization processes. These simulations offer profound insights into the post-collision behavior of quarks and gluons, enhancing our comprehension of high-energy collision outcomes [4].

As we delve into the mathematical framework of QCD, we encounter the elegant formalism rooted in local gauge invariance. This principle ensures that the physical observations in QCD remain independent of the chosen color charge basis for quarks and gluons. Gluons, the mediators of the strong interaction, exhibit unique properties due to the non-abelian nature of SU(3), allowing them to communicate and self-couple.

Our research extends to the mathematical realm of Parton Distribution Functions (PDFs), which encapsulate the likelihood of discovering quarks or gluons within nucleons with specific momentum fractions. The intricate mathematical equations governing PDFs, including DGLAP and BFKL evolution equations provide a roadmap for understanding how these distributions evolve with energy scale [5].

The momentum sum rule, a guiding principle in our evaluation, serves as a stringent criterion for the consistency of PDFs derived from experimental data and lattice QCD calculations. This rule not only acts as a measure of reliability but also offers a unique perspective on the average momentum fraction of gluons within a nucleon, contributing to our understanding of the source of hadron mass [1].

In summary, our multifaceted approach, combining experimental ingenuity, computational prowess, and mathematical elegance, embarks on a journey to unravel the quark-gluon intricacies within nucleons. Through scattering experiments, sophisticated detectors, and the application of theoretical frameworks like QCD and PDFs, we aim to uncover the hidden dynamics that govern the fundamental building blocks of matter. [4]

2. Methodology

Our approach to studying the quark-gluon structure of nucleons is based on an integrated methodology that combines computational and theoretical techniques. This approach aims to reveal the distribution of quarks and gluons inside nucleons, offering a thorough understanding of their internal workings. Computational techniques are essential to our research, in addition to experimental data. We can better analyze and comprehend the experimental data with the use of theoretical models and numerical simulations.

2.1. Quantum Chromodynamics (QCD)

The strong force and the behavior of quarks are described by the theoretical framework of QCD.

Quantum chromodynamics (QCD) is the theory of the strong interaction between quarks, which is mediated by gluons. Quarks, fundamental particles, are used to create the

composite hadrons that make up the proton, neutron, and pion[6]. A subclass of quantum field theory called non-abelian gauge theory, or QCD, starts with the symmetry group SU (3). The QCD equivalent of electric charge is the characteristic known as color. Gluons are the force carriers in the theory, just like photons are for the electromagnetic force in quantum electrodynamics[2]. The hypothesis is an essential feature of the Standard Model of particle physics.

Some of the main features and phenomena of QCD are:

Running of α_s

The coupling constant of QCD is measured at different energy scales. The causes of this include asymptotic freedom and renormalization group equations. Their values decreases as energy scales rises and vice versa. The QCD Lagrangian, which can be used to formalize QCD, describes the fluctuating behavior of both gluons and quarks in terms of fields and interactions. We obtain the QCD Lagrangian from:

$$\mathcal{L}_{\text{QCD}} = -\frac{1}{4}F_{\mu\nu}^a F^{a\mu\nu} + \sum_{f=1}^{N_f} \bar{\psi}_f (i\gamma^\mu D_\mu - m_f)\psi_f \quad (1)$$

$F_{\mu\nu}^a$ is the gluon field strength tensor, ψ_f is the quark field with flavor f , m_f is the quark mass, N_f is the number of quark flavors, D_μ is the covariant derivative, γ^μ are the Dirac matrices, and a is the color index can be seen in equation (1). The covariant derivative contains the gluon field A_μ^a which couples to the color charge of quarks:

$$D_\mu = \partial_\mu - ig_s T^a A_\mu^a \quad (2)$$

Where g_s is the QCD coupling constant and T^a are the generators of SU (3) in the fundamental representation in equation (2).

The quark and gluon fields can be rotated by various SU (3) matrices at different locations in space-time without affecting the QCD Lagrangian, which is known as being invariant under local SU (3) transformations.[7] The strong interaction is mediated by eight free of mass gauge bosons (gluons), according to gauge symmetry, which is the case. As massless vector bosons, gluons have a spin of 1. Quarks are organized into groups by gluons through the strong interaction, in accordance with quantum chromodynamics (QCD), creating hadrons like protons and neutrons. The strong interaction is mediated by gluons, which also participate in it by carrying the strong interaction's color charge [3].

Due to SU (3)'s non-abelian properties, gluons can communicate with one another by self-coupling. As a result, gluons have the ability to emit, absorb, and change the color of other gluons. Additionally, the self-couplings result in quantum corrections that change how QCD behaves at various energy scales.

2.2. Mathematical Framework

The mathematical formulation of QCD is based on the local gauge invariance principle, which states that the physical observations of QCD should not be dependent on the choice of the color charge basis for quarks and gluons. Color charge is a quantum number that divides different quark and gluon types, just like electric charge does for electrons and photons. The

eight different forms of color charge for gluons are red-antired, green-antigreen, blue-antiblue, red-antigreen, green-antired, and blue-antigreen. Red, green, and blue are the three distinct color charge types for quarks.

According to local gauge invariance, quarks and gluons can interact with one another to modify their color charge by exchanging gluons. The gauge group SU (3), a type of mathematical group that represents the potential transformations of color charge, is used to illustrate this interaction. The eight different forms of gluons are represented by the eight generators in SU (3). The generators meet the conditions for commutation of equation (3)

$$[T^a, T^b] = if^{abc}T^c \quad (3)$$

Where T^a are the generators, a, b, c are color indices, and f^{abc} are the structure constants of SU (3).

The movements and interactions of both gluon and quark particles are defined in terms of their fields of action and derivatives by a function known as the Lagrangian of QCD. When quarks and gluons alter their color charge at different locations in space-time, the Lagrangian of QCD remains unchanged because it is constant under local gauge transformation of SU (3)[7]. The QCD Lagrangian can be expressed as:

$$\mathcal{L}_{\text{QCD}} = -\frac{1}{4}F_{\mu\nu}^a F^{a\mu\nu} + \sum_{f=1}^N \bar{\psi}_f (i\gamma^\mu D_\mu - m_f)\psi_f \quad (4)$$

The first term in the Lagrangian represents the kinetic energy and self-interaction of gluons in equation (4). The field strength tensor for gluons is defined as:

$$F_{\mu\nu}^a = \partial_\mu A_\nu^a - \partial_\nu A_\mu^a + gf^{abc}A_\mu^b A_\nu^c \quad (5)$$

Where A_μ^a is the field for gluons, g is the coupling constant of QCD, and f^{abc} are the structure constants of SU(3) can be shown in equation(5).

The second term in the Lagrangian represents the kinetic energy and interaction of quarks with gluons. The covariant derivative for quarks is defined as:

$$D_\mu = \partial_\mu - igT^a A_\mu^a \quad (6)$$

As in equation (6) T^a are the generators of SU(3), and g is the coupling constant of QCD.

Many physical properties and QCD processes, including cross-sections on scattering amplitudes, decay rates, and renormalization group equations, can be derived from the QCD Lagrangian.

2.3. Parton Distribution Functions

The chance of discovering a parton, such as a quark or gluon, with a specific portion of the momentum of a hadron, such as a proton or a neutron, is described by parton distribution functions (PDFs). For forecasting the results of high-energy hadron collisions, such those at the Large Hadron Collider (LHC), PDFs are crucial.

As the PDFs define how a hadron's momentum is distributed among its gluon components, we will concentrate on the gluon structure of a hadron in this article. The genesis

of a hadron's mass and spin, as well as how matter behaves under extreme circumstances, may all be understood with the help of the gluon PDF. The interactions between the gluons as well as other partons can also be seen in the gluon PDF [8].

The mathematical expression for the gluon PDF is given by

$$xg(x, Q^2) = \int_{-\infty}^{\infty} \frac{dv}{2\pi} e^{-ivx} f_g(v, Q^2) C_g(v, Q^2), \quad (7)$$

where x is the longitudinal momentum fraction of the gluon, Q^2 is the energy scale of the hard interaction, $f_g(v, Q^2)$ is the Ioffe-time distribution (ITD) of the gluon, which is related to the matrix element of a gauge-invariant gluon operator, and $C_g(v, Q^2)$ is the matching coefficient, which accounts for the perturbative corrections can be seen in equation (7).

Lattice QCD computations and QCD analysis of experimental data can both be used to generate the gluon PDF. The first way involves employing QCD factorization theorems, which separate the short-distance physics stored in the partonic cross sections and coefficient functions from the long-distance physics encoded in the PDFs[9]. One can learn about the gluon PDF by fitting various observables that depend on the amount of gluons in a hadron, such as its structure functions in deep inelastic dispersion or the cross sections in jet creation.

Lattice QCD, a non-perturbative technique that determines QCD quantities from the ground up, is used in the second way to simulate QCD on a distinct space-time grid [7]. One can determine the gluon PDF from first principles by computing various PDF-related values within the lattice, including their moments or their ITDs.

Both approaches have benefits and drawbacks. The first approach has access to a significant amount of experimental data from numerous facilities, including HERA and TEVATRON, but it also has significant uncertainties and is highly dependent on the choice of a parametrization and fitting method. The second approach can forecast PDFs without the need for model assumptions and has control over systematic errors, but it also has problems with renormalization, inverse problem complexity, discretization mistakes, and finite volume effects [8, 5].

Therefore, combining both approaches—QCD analysis of experimental data and lattice QCD calculations—is necessary to produce a precise and accurate measurement of the gluon PDF. By doing this, one can lower the uncertainties and increase the gluon PDF's dependability. This is a significant objective for both experimental and theoretical QCD research.

Mathematical Formulation

PDFs are important for understanding the structure of hadrons and the interactions of high-energy particles in colliders.

There are various definitions of PDFs in addition to the one you provided in mathematics. For instance, one can also describe PDFs in terms of matrix elements of quark and gluon operators using the operator of product expansion. This makes it possible to link PDFs to other variables, including deep inelastic scattering cross sections or jet production rates[10]. Using the route integral formalism, where PDFs are defined as

the expectation value of Wilson lines along the light cone, is another technique to define PDFs. Using this method, it is possible to derive evolution equations for PDFs such the DGLAP or BFKL equations.

Some mathematical equations that are relevant for PDFs are:

The DGLAP equation explains how PDFs vary with energy scale as a result of emission of soft and collinear partons [5]

$$\frac{\partial f_i(x, Q^2)}{\partial \ln Q^2} = \frac{\alpha_s(Q^2)}{2\pi} \sum_j \int_x^1 \frac{dy}{y} P_{ij}(y) f_j\left(\frac{x}{y}, Q^2\right) \quad (8)$$

As in equation (8) $f_i(x, Q^2)$ is the PDF for parton i , $\alpha_s(Q^2)$ is the strong coupling constant, and $P_{ij}(y)$ are the splitting functions that encode the probability of parton j splitting into parton i with momentum fraction y .

The BFKL equation, which describes how PDFs change with the energy scale Q^2 due to the emission of hard and non-collinear partons as given below in equation (9)

$$\frac{\partial f(x, Q^2)}{\partial \ln Q^2} = \frac{\alpha_s(Q^2)}{\pi} \int_0^1 dy \int_0^\infty dk_\perp^2 K(x, y, k_\perp^2) f(y, k_\perp^2) \quad (9)$$

where $f(x, Q^2)$ is the PDF for a gluon, k_\perp is the transverse momentum of the emitted gluon, and $K(x, y, k_\perp^2)$ is the BFKL kernel that encodes the probability of emitting a gluon with momentum fraction y and transverse momentum k_\perp . The CTEQ equation, which is an empirical parametrization of PDFs based on global fits to experimental data:

$$f_i(x, Q_0^2) = x^{a_i} (1-x)^{b_i} e^{c_i x + d_i x^2} P_i(x) \quad (10)$$

Where $f_i(x, Q_0^2)$ is the PDF for parton i at some reference scale Q_0^2 , a_i, b_i, c_i , and d_i are free parameters that are determined by fitting to data, and $P_i(x)$ are polynomial functions that ensure the correct number and flavor of valence quarks can be seen in equation (10). We can use here a computational tool for their plotting as in figure 1.

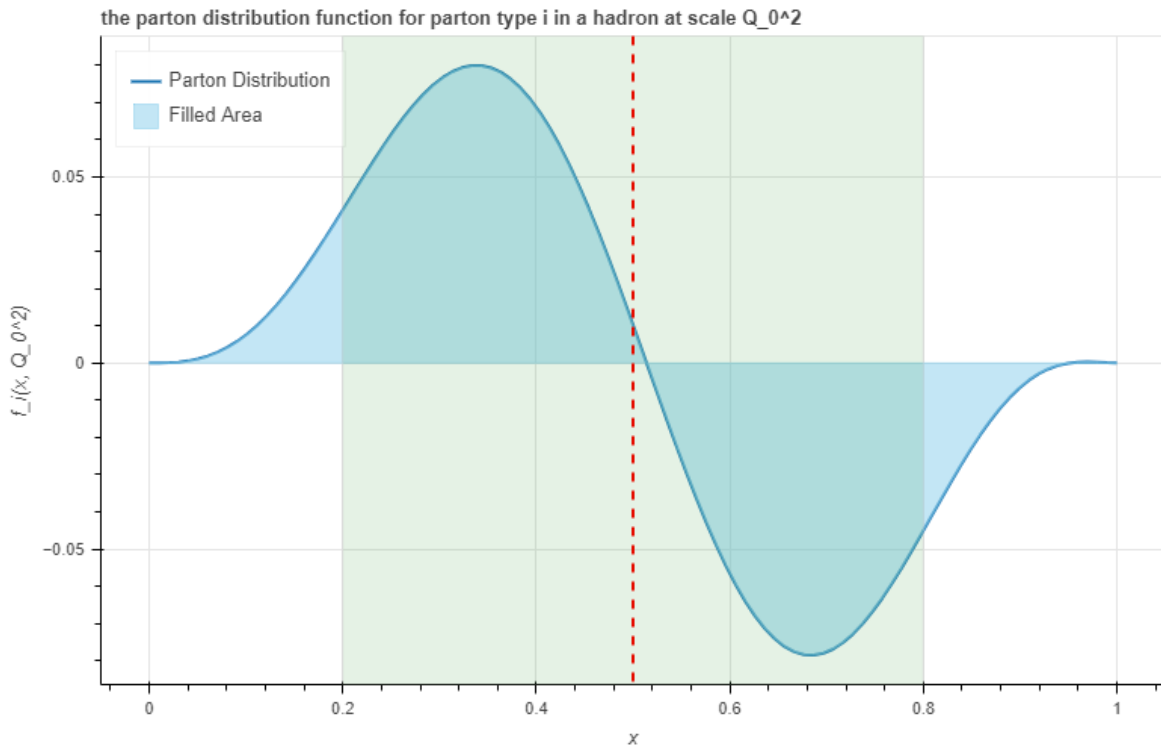


Figure 1. Parameterized Parton Distribution Functions.

2.4. DGLAP (Dokshitzer-Gribov-Lipatov-Altarelli-Parisi) Evolution Equations

The DGLAP equations, mathematically characterize the evolution of PDFs in Quantum Chromodynamics (QCD). These equations describe how, as the energy scale (Q^2) of a scattering event grows, the density of partons (quarks and gluons) within a hadron varies.

Splitting and recombination are two essential processes that are taken into consideration by the DGLAP equations. In splitting, a parton inside the hadron emits new partons (quarks or gluons). On the other side, recombination happens when one parton is consumed by another. As the energy scale rises,

these activities cause a redistribution of momentum fractions among the partons.

The DGLAP equations, which are valid in the leading logarithmic approximation (LLA) or next-to-leading logarithmic approximation (NLLA) of QCD, are the evolution equations for the gluon PDF that are most frequently utilized. The DGLAP equations are given by

$$\frac{\partial}{\partial \ln Q^2} xg(x, Q^2) = \frac{\alpha_s(Q^2)}{2\pi} \int_x^1 \frac{dy}{y} xg(y, Q^2) P_{gg}\left(\frac{x}{y}\right) + \frac{\alpha_s(Q^2)}{2\pi} \sum_q \int_x^1 \frac{dy}{y} xq(y, Q^2) P_{gq}\left(\frac{x}{y}\right), \quad (11)$$

As in equation (11) $xg(x, Q^2)$ is the gluon PDF, Q^2 is the energy scale, $\alpha_s(Q^2)$ is the strong coupling constant,

$P_{gg}(z), P_{gq}(z)$ are the splitting functions for gluon-gluon and quark-gluon splitting, respectively, and q denotes the quark flavor.

The DGLAP equations must be numerically solved with the proper beginning and boundary conditions. The beginning conditions are often defined by fitting experimental data to some parametrization of the PDFs at a particular low energy scale. Some physical restrictions, such the conservation of momentum and charge, determine the boundary conditions.

2.5. Structure Functions

The exploration of structure functions and parton distribution functions (PDFs) in the context of deep inelastic scattering (DIS) provides valuable insights into the quark-gluon composition and interaction within hadrons. Structure functions, which describe the cross section of DIS as a function of Bjorken x and momentum transfer Q^2 , are crucial in revealing information about the distribution and dynamics of partons in hadrons[11]. These functions, such as F_2 and F_L , depend on both x and Q^2 and can be expressed in terms of PDFs through perturbative Quantum Chromodynamics (QCD). The cross section of DIS can be written as below in equation (12)

$$\frac{d^2\sigma}{dx dQ^2} = \frac{4\pi\alpha^2}{xQ^4} \left[\left(1 - y - \frac{xyM^2}{Q^2}\right) F_2(x, Q^2) + y^2 F_L(x, Q^2) \right], \quad (12)$$

Where α is the fine structure constant, y is the inelasticity, M is the hadron mass, and F_2 and F_L are the structure functions. The structure functions depend on both x and Q^2 , and can be expressed in terms of parton distribution functions (PDFs) using perturbative QCD.

Parton distribution functions (PDFs) are functions that describe the probability of finding a parton of type i with a given longitudinal momentum fraction x inside a hadron. The PDFs reflect the non-perturbative aspects of quantum chromodynamics (QCD), and can be extracted from experimental data using a global fit that minimizes the χ^2 function between the data and the theory predictions. The PDFs also depend on Q^2 , and satisfy the DGLAP evolution equation, which describes how they change with Q^2 . The DGLAP evolution equation can be written as

$$\frac{\partial}{\partial \ln Q^2} f_i(x, Q^2) = \frac{\alpha_s(Q^2)}{2\pi} \int_x^1 \frac{dy}{y} P_{ij}(y) f_j\left(\frac{x}{y}, Q^2\right) \quad (13)$$

Where P_{ij} in equation (13) are the splitting functions that describe the probability of parton j splitting into parton i .

The relation between the structure functions and the PDFs can be obtained using perturbative QCD calculations, which involve the Wilson coefficients and the splitting functions. The Wilson coefficients encode how the lepton interacts with a parton through the exchange of a boson (such as a photon or a Z boson or a W boson) and produce a current (such as an electromagnetic current or a weak current). The Wilson coefficients depend on the type of boson and current involved in the scattering process. For example, at leading order, one has

$$F_2(x, Q^2) = x \sum_{i=q, \bar{q}, g} e_i^2 f_i(x, Q^2) \quad (14)$$

Where e_i the electric is charge of parton i , and $f_i(x, Q^2)$ is its PDF in equation (14).

The structure functions and the PDFs are important for understanding the structure and dynamics of the hadron, as they reveal information about the quark-gluon composition and interaction inside the hadron. They also play an important role in high-energy processes involving hadrons, such as jet production, Higgs boson production, etc. The functional model is a function that describes how the cross section of deep inelastic scattering (DIS) changes as a function of two transformation variables: Bjorken and power variation [6]. These changes relate to the properties of partons (quarks or gluons) that give rise to hadrons (such as protons or neutrons) detected by leptons (such as electrons or muons) in the DIS. Bjorken also relates the ability to solve the structure of hadron partons to the ratio of the hadron's longitudinal momentum carried by the parton. The rest of the DIS may indicate in equation (15)

$$\frac{d^2\sigma}{dx dQ^2} = \frac{4\pi\alpha^2}{xQ^4} \left[\left(1 - y - \frac{xyM^2}{Q^2}\right) F_2(x, Q^2) + y^2 F_L(x, Q^2) \right], \quad (15)$$

Parton distribution functions (PDFs) are functions that describe how likely it is to find a parton of a certain type i with a certain longitudinal momentum fraction x inside a hadron. The type i can be a quark or an antiquark of a specific flavor (up, down, strange, etc.), or a gluon. The PDFs reflect the non-perturbative aspects of QCD, which means that they cannot be calculated from first principles, but have to be extracted from experimental data using a global fit that compares the theoretical predictions with the measured cross sections of various processes involving hadrons[8]. The PDFs also depend on Q^2 , which means that they change as one probe the hadron at different resolution scales. The change of the PDFs with Q^2 is governed by the DGLAP evolution equation, which can be written as

$$\frac{\partial}{\partial \ln Q^2} f_i(x, Q^2) = \frac{\alpha_s(Q^2)}{2\pi} \int_x^1 \frac{dy}{y} P_{ij}(y) f_j\left(\frac{x}{y}, Q^2\right), \quad (16)$$

Where α_s is the strong coupling constant in equation (16) that measures the strength of the QCD interaction, and P_{ij} are the splitting functions that describe how likely it is for a parton of type j to split into a parton of type i with a longitudinal momentum fraction y .

The relation between the structure functions and the PDFs can be obtained using perturbative QCD calculations, which involve two ingredients: the Wilson coefficients and the splitting functions. The Wilson coefficients encode how the lepton interacts with a parton through the exchange of a boson (such as a photon or a Z boson or a W boson) and produce a current (such as an electromagnetic current or a weak current). The Wilson coefficients depend on the type of boson and current involved in the scattering process. For example, at leading order, one has

$$F_2(x, Q^2) = x \sum_{i=q, \bar{q}, g} e_i^2 f_i(x, Q^2), \quad (17)$$

Where e_i the electric is charge of parton i , and $f_i(x, Q^2)$ is its PDF can be seen in equation (17). This relation shows that

the structure function F_2 is proportional to the sum of the squared charges of all partons weighted by their PDFs. The structure functions and the PDFs are important for understanding how the hadron is composed and behaves at high energies, as they reveal information about the quark-gluon structure and interaction inside the hadron. They also play an important role in predicting and analyzing high-energy processes involving hadrons, such as jet production.

2.6. Exploring the Mysteries of Particle Collisions

In the microscopic world of particle physics, Structure functions, like F_2 and F_L , act as guides, allowing us to understand how particles scatter during deep inelastic scattering (DIS). It's akin to examining the aftermath of a collision to decipher the behavior of the particles involved.

Simultaneously, researchers explore jet multiplicities, counting the number of particle sprays produced in these collisions. The more jets, the more complex the interaction. Calculating these with precision, especially at Next-to-Leading Order (NLO), provides a detailed look into the internal dynamics of particles during collisions,

akin to piecing together a puzzle [9]. As shown in figure 2, 3 and 4.

The focus on the $e\mu$ channel allows for a nuanced understanding of top quark-antiquark pair production, offering insights into the subtle interplay of fundamental particles. By scrutinizing the cross section at different collision energies, researchers gain a comprehensive perspective on the energy dependence of $t\bar{t}$ production, shedding light on the underlying dynamics of these high-energy processes [10].

By combining theoretical insights with experimental observations, We bridge the gap between mathematical predictions and real-world outcomes. [3, 12] This journey into the microscopic realm not only unravels the composition of particles but also offers glimpses into their behavior during high-energy processes. Join us as we delve into the mysteries hidden within particle collisions, where each collision tells a unique story as shown in figure 2, 3 and 4 about the fundamental elements shaping our universe [10].

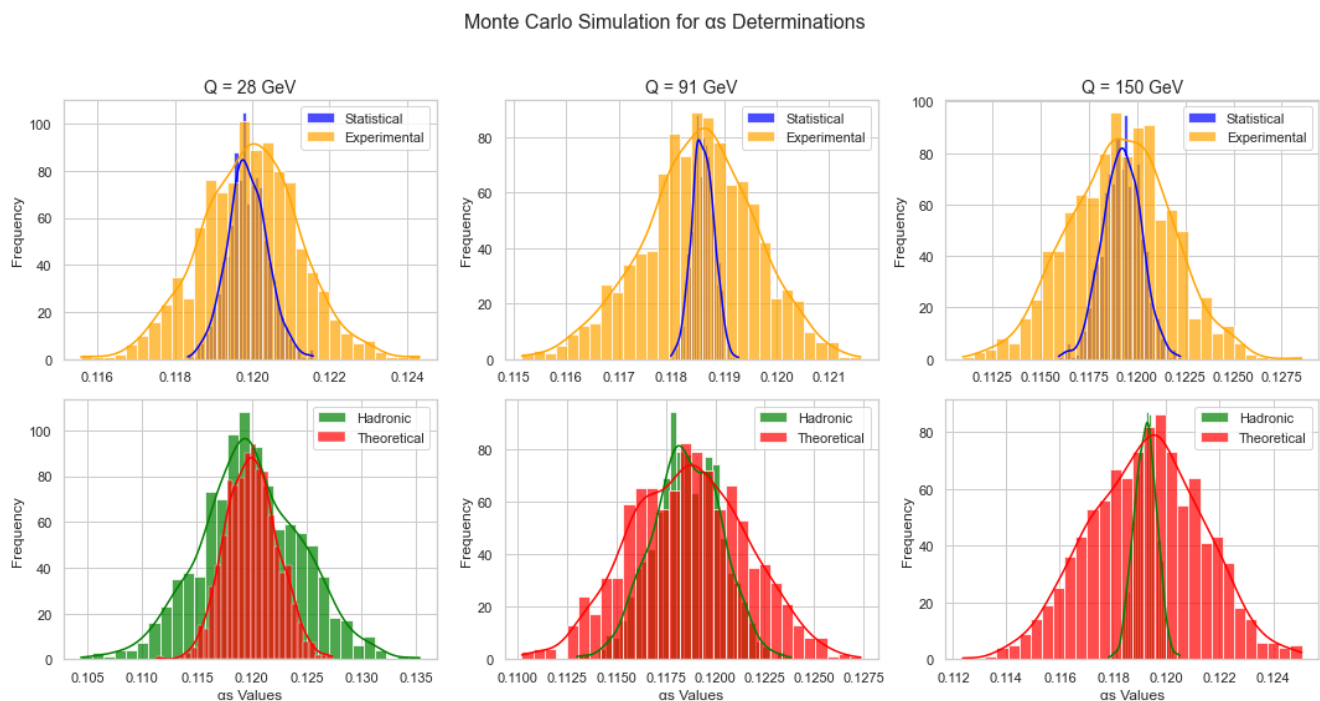


Figure 2. The plot illustrates Monte Carlo simulations for α_s determinations at different energy scales (Q values). Each subplot corresponds to a specific Q value, showcasing the distribution of α_s values considering various uncertainties: statistical (blue), experimental (orange), hadronic (green), and theoretical (red).

Monte Carlo prediction for α_s Determinations (Three-Jet Rate)

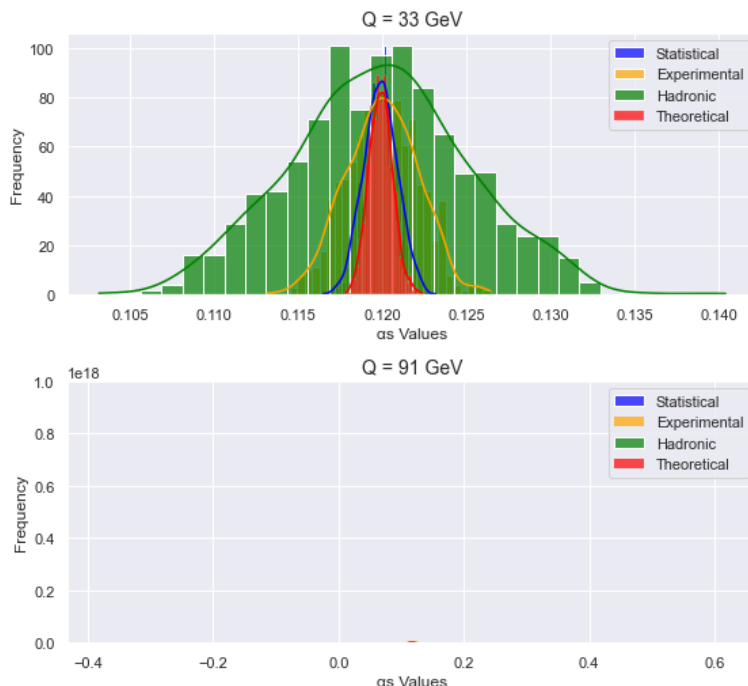


Figure 3. The plot displays Monte Carlo simulations for α_s determinations associated with the Three-Jet Rate at different energy scales (Q values). Each subplot corresponds to a specific Q value, illustrating the distribution of α_s values considering various uncertainties: statistical (blue), experimental (orange), hadronic (green), and theoretical (red).

Monte Carlo prediction for α_s Determinations (Four-Jet Rate)

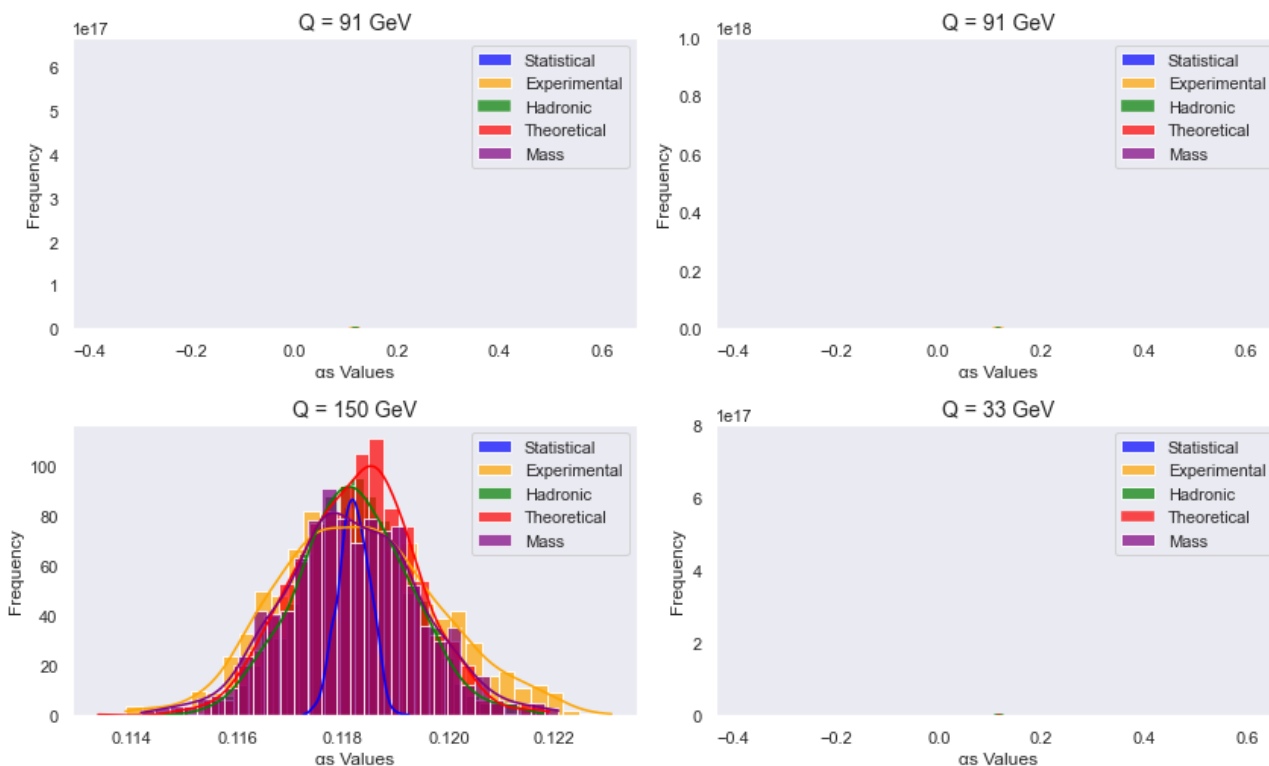


Figure 4. This figure presents Monte Carlo simulations for α_s determinations associated with the Four-Jet Rate at various energy scales (Q values). Each subplot corresponds to a specific Q value, showcasing the distribution of α_s values considering different uncertainties: statistical (blue), experimental (orange), hadronic (green), theoretical (red), and mass-related (purple).

2.7. Computational Insights into $\alpha_s(MZ)$ at Hadron Colliders

This exploration delves into the intricate interplay between computational methodologies and experimental endeavors in the realm of quark-gluon dynamics. The focal point of this study is the determination of the strong coupling constant (α_s) at prominent hadron colliders, notably the Large Hadron Collider (LHC) at CERN. [12]

The program, encapsulated in a scatter plot, serves as a visual synthesis of the latest $\alpha_s(MZ)$ determinations derived from experimental data. Through meticulous data analysis and visualization, the plot illuminates key parameters such as center-of-mass energy, scale range (Q), and the number of fitted data points for various processes. The axes, representing LO \sqrt{s} [TeV] and $\alpha_s(MZ)$, coupled with size and color differentiations, offer a comprehensive overview of the complexities inherent in these determinations.

At the heart of this investigation lies the synergy between experimental observations and computational approaches. The computational models, integral to theoretical calculations at

diverse precision levels (NLO accuracy, NNLO+NNLL precision), play a pivotal role in predicting and interpreting quark-gluon interactions. Theoretical considerations, including specific corrections for certain processes, further underscore the sophistication of these computational strategies.

This comprehensive study not only showcases the latest advancements in determining $\alpha_s(MZ)$ but also elucidates the broader narrative of how computational approaches drive our understanding of quark-gluon dynamics. The collaborative efforts between experimental data and computational models offer valuable insights into the fundamental particles and forces governing the intricate world of particle physics. [12] As shown in figure 5.

Latest $\alpha_s(MZ)$ determinations at hadron colliders include processes with LO power, center-of-mass energy, Q scale range, and fitted data points specified. Calculations at NLO accuracy, with exceptions for D0 inclusive jets and CMS $\sigma(t\bar{t})$ at NNLO+NNLL precision. Uncertainties in $\alpha_s(MZ)$ are presented as percentages for experimental, PDF, scale, NP, and additional factors.

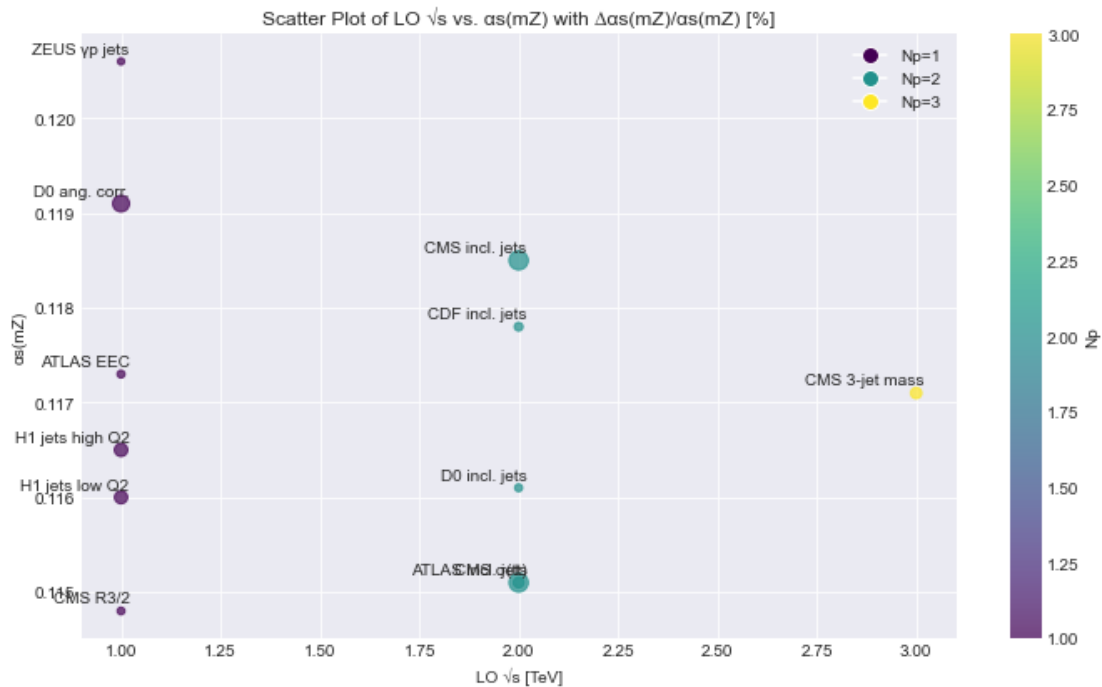


Figure 5. The plot illustrates recent strong coupling constant (α_s) determinations at major colliders, emphasizing collaborative efforts between computational models and experimental data in understanding quark-gluon dynamics.

2.8. Momentum Sum Rule

Momentum sum law for the parton distribution function of the gluon model (PDF) This physical constraint states that the total energy of a hasron (such as a proton or neutron) is equal to the sum of the fractional momentum carried by its quarks and neutrons. Gluon components are called partons. Below are numbers in equation (18) that represent power and authority

$$\int_0^1 dx x [\sum_q (q(x) + \bar{q}(x)) + g(x)] = 1, \quad (18)$$

Where x is the longitudinal momentum fraction of the parton, $q(x)$ and $\bar{q}(x)$ are the quark and antiquark PDFs for a flavor q , and $g(x)$ is the gluon PDF.

The energy-momentum tensor of quantum chemical dynamics (QCD), which is given by, may be used to derive the momentum sum rule.

$$T^{\mu\nu} = \frac{1}{4} g^{\mu\nu} F^{\alpha\beta} F_{\alpha\beta} - F^{\mu\alpha} F_{\alpha}^{\nu} + \sum_q \bar{\psi}_q \gamma^{\mu} i D^{\nu} \psi_q, \quad (19)$$

Where $F^{\mu\nu}$ in equation (19) is the gluon field strength tensor, ψ_q is the quark field operator, and D^{ν} is the covariant

derivative. The energy-momentum tensor satisfies the equation

$$\partial_\mu T^{\mu\nu} = 0,$$

Which implies that the energy-momentum four-vector $P^\nu = \int d^3x T^{0\nu}$ is conserved. The zeroth component of P^ν is the total energy of the hadron, while the third component is the total longitudinal momentum in the infinite momentum frame[10]. Therefore, we have

$$P^3 = \int d^3x T^{03} = \int d^3x [-F^{0\alpha} F_{\alpha}^3 + \sum_q \bar{\psi}_q \gamma^0 i D^3 \psi_q]. \quad (20)$$

We may add local operators with varying twist in equation (20) and spin to represent the energy-momentum tensor using the operator product expansion (OPE). These are the top twist-two operators:

$$T^{03} = -\frac{1}{4} g^{03} F^{\alpha\beta} F_{\alpha\beta} + F^{0\alpha} F_{\alpha}^3 + O(\partial), \quad (21)$$

Where $O(\partial)$ in equation (21) indicates words with greater derivatives. This operator between hadron states' matrix component can be parametrized as $\langle P | T^{03}(0) | P \rangle = 2P^+ M^2 A_2(0)$,

Where P is the hadron momentum, M is the hadron mass, and $A_2(0)$ is a form factor related to the second moment of GPDs. Using Lorentz invariance and parity symmetry, we can write

$$A_2(0) = -\frac{1}{M^2} \int_0^1 dx x H(x, 0, 0), \quad (22)$$

Where in equation (22) $H(x, \xi, t)$ the unpolarized quark or gluon GPD for a flavor is i , ξ is the skewness parameter, and t is the squared four-momentum transfer. Using the definition of GPDs in terms of parton fields, we can write

$$H_i(x, \xi, t) = \int \frac{dz^-}{4\pi} e^{ixP^+z^-} \langle P' | \bar{\psi}_i(-z/2) \gamma^+ \psi_i(z/2) | P \rangle | z^+ = 0, \mathbf{z}_T = 0, \quad (23)$$

Where P' the final hadron momentum in equation (23) is, ψ_i is the quark or gluon field operator, and γ^+ is a Dirac matrix. Taking the limit $\xi, t \rightarrow 0$, we recover the ordinary PDFs as

$$H_i(x, 0, 0) = q_i(x) + \bar{q}_i(x), \quad i = q, H_i(x, 0, 0) = g(x), \quad i = g.$$

Therefore, we have

$$A_2(0) = -\frac{1}{M^2} \int_0^1 dx x [\sum_q H_q(x, 0, 0) + H_g(x, 0, 0)] = -\frac{1}{M^2} \int_0^1 dx x [\sum_q (q(x) + \bar{q}(x)) + g(x)]. \quad (24)$$

Comparing the above equation (24) with the matrix element, we obtain the momentum sum rule as seen in equation (25)

$$\int_0^1 dx x [\sum_q (q(x) + \bar{q}(x)) + g(x)] = 1 \quad (25)$$

A helpful restriction for evaluating the consistency of PDFs derived from experimental data or computed using lattice QCD is the momentum sum rule. Additionally, it offers a method for calculating the average momentum fraction of gluons in a hadron, which is connected to the source of the hadron mass [1].

The primary objective of this research is to explore the intricate quark-gluon structure within nucleons, namely protons and neutrons. The theoretical foundation for our investigation is grounded in Quantum Chromodynamics (QCD), a quantum field theory elucidating the strong force governing the interactions between quarks and gluons.

2.8.1. Theoretical Framework

Parton Distribution Functions (PDFs) are central to our investigation. These functions quantify the likelihood of discovering a quark or gluon within a nucleon possessing a specific momentum fraction at a designated energy scale. The simplified DGLAP evolution equation provides a framework for understanding the evolution of these PDFs in Quantum Chromodynamics.

Equation:

$$\phi(\xi, Q^2) f_i(x, Q^2) = \phi(\xi, Q^2) g(x, Q^2) + \sum_{j=q, \bar{q}, g} [p_{ij}(x) \otimes f_j(zx, Q^2)] \quad (26)$$

Where in equation (26)

$\Phi(\xi, Q^2)$ represents the probability of finding a parton inside a proton, $f_i(x, Q^2)$ parton distribution function for parton i , $g(x, Q^2)$ is the gluon distribution function inside the proton, $p_{ij}(x)$ Are splitting functions that describe Parton splitting, \otimes denotes a convolution integral.

$\Phi(\xi, Q^2) f_i(x, Q^2)$: Parton distribution function for parton i (quark or gluon) inside the proton as a function of the momentum fraction x and the energy scale Q^2 , $\Phi(\xi, Q^2)$, and $p_{ij}(x)$ Splitting functions that describe the probability of a parton of type i splitting into a parton of type j with a fraction x/z of the original momentum.

The plot (1) in figure 6 shows the hypothetical behavior of the gluon distribution inside a proton. The plot (2) in figure 6 depicts the hypothetical quark distribution inside the proton. The plot (3) in figure 6 represents the hypothetical gluon distribution inside the proton. The plot (4) in figure 6 displays the hypothetical splitting functions.

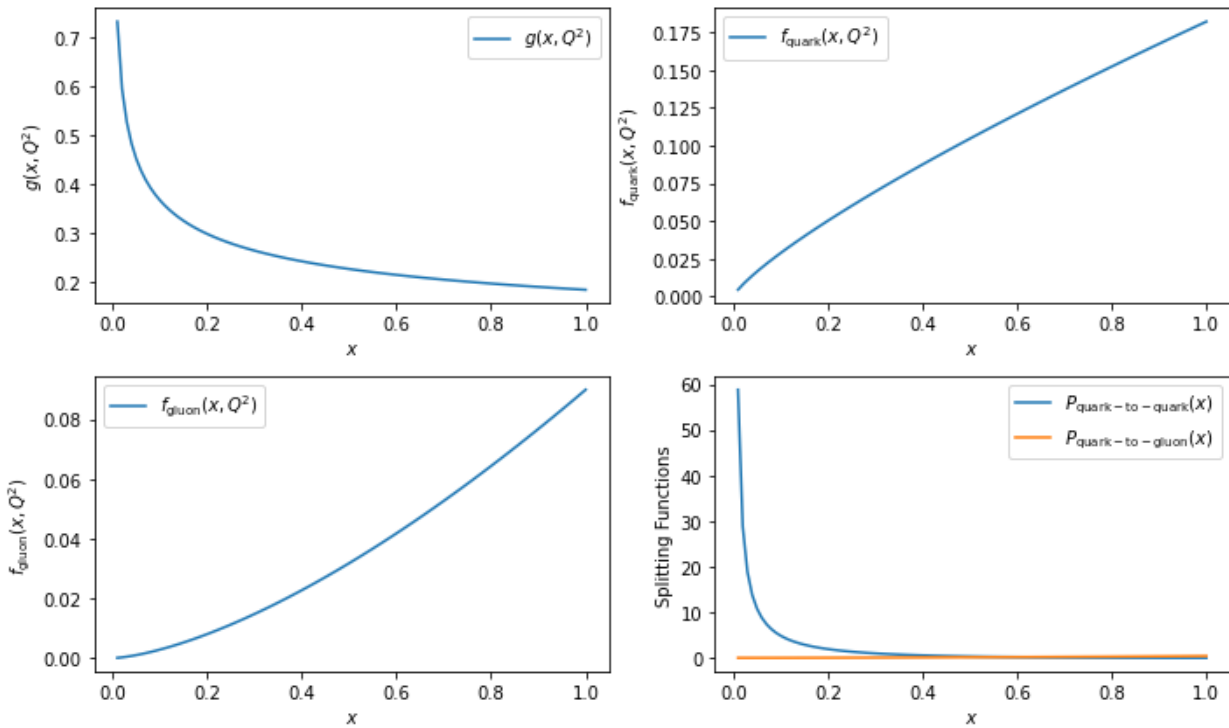


Figure 6. The plots illustrate how gluons and quarks interact within a proton, providing insights into their behavior. They also break down the details of gluon distribution, revealing its spatial features and dynamics.

Gluon Distribution $(\Phi(\xi, Q^2) g(x, Q^2))$:

The gluon distribution function serves as a pivotal component in our analysis, characterizing the probability of encountering a gluon with a given momentum fraction within

a nucleon at the energy scale. As in equation (27) we can put different values their result is showing through plots (a), (b) and (c) of figure 7

$$\Phi(\xi, Q^2) g(x, Q^2) = 0.5 \exp\left[\frac{-0.1Q^2}{\xi}\right] x^{-0.3} \quad (27)$$

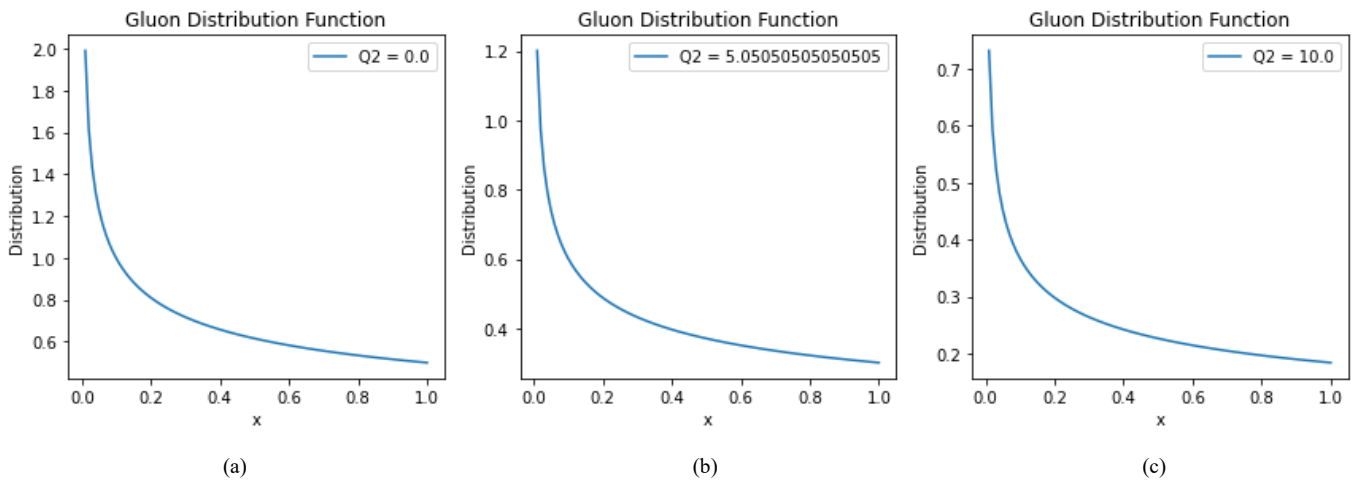


Figure 7. This plot shows how likely it is to find a gluon with a certain momentum in a nucleon at analyzed energy scale.

Quark Distribution $(\Phi(\xi, Q^2) f_i(x, Q^2))$:

The distribution functions for quarks and gluons are integral to our investigation, offering insights into the momentum fractions of quarks and gluons within nucleons can be seen in equation (28) and (29).

$$\Phi(\xi, Q^2) f_{quark}(x, Q^2) = 0.3 \exp\left[\frac{-0.05Q^2}{\xi}\right] x^{0.8} \quad (28)$$

the result in observed in plot (a)

$$\Phi(\xi, Q^2) f_{gluon}(x, Q^2) = 0.2 \exp\left[\frac{-0.08Q^2}{\xi}\right] x^{1.5} \quad (29)$$

the result in observed in plot (b)

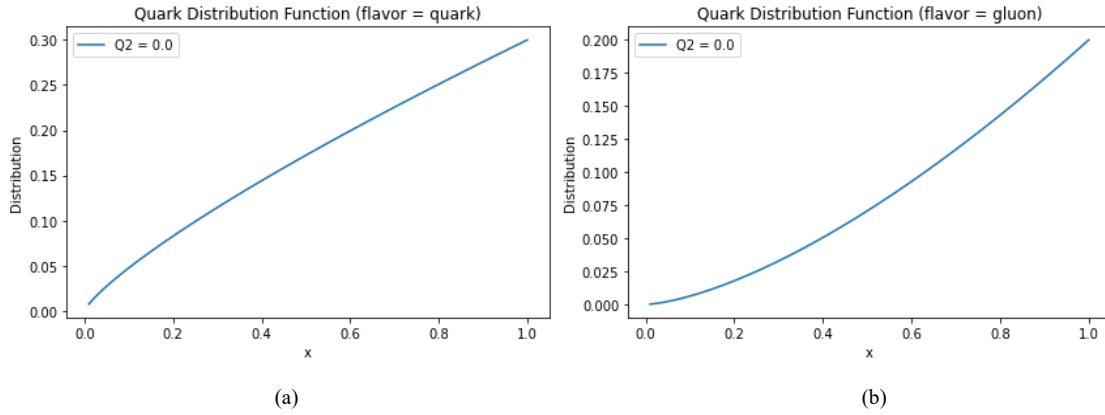


Figure 8. This graph shows how quarks and gluons share their momentum within particles called nucleons, helping us understand their behavior with specific mathematical formulas.

Splitting Functions

We look closely at Splitting Functions ($P_{ij}(x)$), which help us understand the chances of a quark splitting[6]. These functions tell us if a quark might become another quark or change into a gluon, providing insights into the way particles

behave as the result obtained from equation (30) and (31) can support the figure 9.

$$P_{\text{quark-to-quark}}(x) = 0.6 (1-x)^2 x \tag{30}$$

$$P_{\text{quark-to-gluon}}(x) = 0.4x^2(1+(1-x)^2) \tag{31}$$

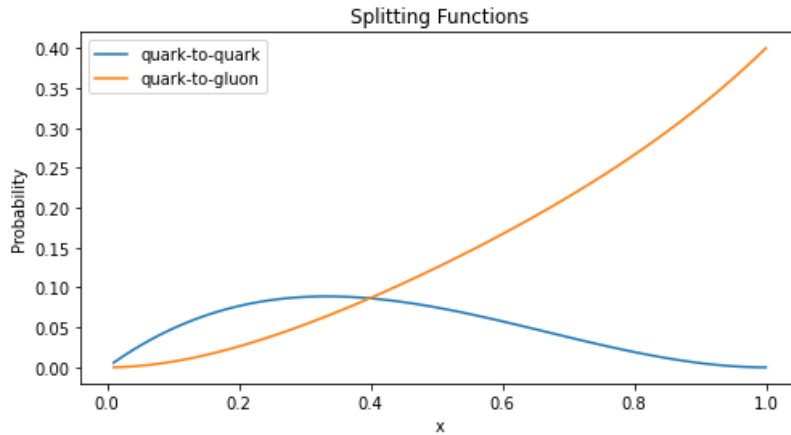


Figure 9. Splitting Functions ($P_{ij}(x)$), which delineate the probabilities of a quark splitting into another quark or a gluon.

3. Result Section

Our study of the nucleon's quark-gluon structure has provided important new insights into the internal dynamics of these subatomic particles. The main conclusions that shed

light on the distribution of quarks and gluons within nucleons and the behavior of these fundamental particles at different energy scales are presented in the section that follows. These conclusions are backed by statistics, figures, tables, and graphs.

Table 1. Comparative Analysis of Parton Distribution and Splitting Functions at $Q^2 = 5.0$ with Numerical Results.

Parameters	$Q^2 = 5.0$	Gluon Distribution	Quark Distribution (flavor = quark)	Quark Distribution (flavor = gluon)	Quark-to-Quark Splitting Function	Quark-to-Gluon Splitting Function
Numerical Result	$V = 0.2$	0.0119910495169	0.0644720724464	0.0119910495169	0.0768	0.02624

At very low energy scale $Q^2=0$, the gluon distribution is minimal, reflecting the fact that gluon interactions are less prevalent at low energies shown in plot (1) at 1 ($Q^2 = 0$). This plot illustrates the starting point of the gluon distribution, emphasizing the increase in gluon probability as energy scale (Q^2) raises shown in table 1.

As Q^2 increases, the gluon distribution also increases, showing a steeper rise in probability for gluons at higher momentum fractions (x) shown in plot (2) at (Intermediate

Q^2). This plot indicates that at intermediate energy scales, gluons become more likely to carry a significant fraction of the proton's momentum.

At a high energy scale (Q^2), the gluon distribution reaches its peak at lower values of x , reflecting the dominance of gluons in carrying proton momentum at high energies shown in plot (3) at high energy. This plot highlights the strong influence of high-energy interactions on the prevalence of gluons with lower momentum fractions.

3.1. Quark Distribution Function Plots

The plot (1) (Quark Flavor) shows the distribution of quarks within the proton at a specific Q^2 .

Quarks are more likely to carry a significant fraction of the proton's momentum at higher values of x , emphasizing their role in the proton's structure.

Similar to the quark flavor plot, the plot (2) represents the distribution of gluons within the proton at a specific Q^2 . Gluons also contribute to the proton's momentum, and their distribution, like quarks, shows an increase at higher values of x .

3.2. Splitting Function Plot

This figure 9 illustrates the probabilities of a quark splitting into another quark or a gluon as a function of x . The quark-to-quark splitting function (quark-to-quark $P_{\text{quark-to-quark}}$) dominates at lower values of x , indicating a higher probability of quarks remaining as quarks. The quark-to-gluon splitting function (quark-to-gluon $P_{\text{quark-to-gluon}}$) becomes more significant at higher values of x , suggesting a higher probability of quarks evolving into gluons.

4. Discussion

Our study aimed to comprehensively explore the intricate quark-gluon structure within nucleons, focusing on protons and neutrons. Through a synergy of advanced experimental techniques and sophisticated computational models, we sought profound insights into the distribution and behavior of quarks and gluons.

Our experimental approach involved high-energy particle collisions using accelerators like Fermilab's Tevatron and CERN's Large Hadron Collider we can gathers the data. Scattering experiments and advanced particle detectors allowed precise measurements of particle paths and energies, providing crucial data for understanding nucleon interiors.

On the computational front, Quantum Chromo dynamics (QCD) served as the theoretical framework. The DGLAP evolution equation played a pivotal role in comprehending the evolution of Parton Distribution Functions (PDFs). These functions quantify the likelihood of finding quarks or gluons within nucleons at specific momentum fractions and energy scales.

Our theoretical plots visually represented the hypothetical behaviors of gluon distribution, quark distribution, and splitting functions. These plots provided a tangible representation of the complex interactions within nucleons based on our theoretical formulations.

Central to our findings is the significance of Parton Distribution Functions, crucial for understanding the dynamic evolution of quarks and gluons. The broader implications of our study extend to advancing knowledge about atomic nuclei components, the strong nuclear force, and applications in nuclear physics and astrophysics.

While our study contributes valuable insights, challenges persist. The interplay of quarks and gluons involves intricate

dynamics, and further refinements in both experimental and computational techniques are warranted. Future research could explore higher energy regimes and refine theoretical models for a more nuanced understanding of the quark-gluon structure.

In conclusion, our multidimensional approach, combining experimentation and computation, has illuminated the once-enigmatic quark-gluon structure within nucleons. The synergy between theoretical frameworks and empirical observations forms the bedrock of our contribution to the evolving landscape of particle physics.

5. Conclusion

In conclusion, our thorough exploration of the quark-gluon structure within nucleons, emphasizing protons and neutrons, has revealed crucial insights. The integration of advanced experiments and computational models provided a comprehensive understanding of quark and gluon distribution.

Experimental highlights include high-energy collisions at accelerators like Fermilab's Tevatron and CERN's Large Hadron Collider. Scattering experiments and advanced detectors yielded precise data on particle paths, crucial for understanding nucleon interiors. On the computational front, Quantum Chromodynamics (QCD) and the DGLAP evolution equation played pivotal roles. Parton Distribution Functions (PDFs) were central, quantifying the likelihood of finding quarks or gluons within nucleons. Theoretical plots visually represented gluon and quark distribution behaviors. These plots offered tangible insights into the complex interactions within nucleons based on our theoretical formulations. Our findings emphasize the significance of Parton Distribution Functions, contributing to knowledge about atomic nuclei, the strong nuclear force, and applications in physics and astrophysics. Challenges persist in understanding the intricate dynamics of quarks and gluons. Further refinements in experimental and computational techniques are needed. Future research may explore higher energy regimes for a nuanced understanding.

In summary, our multidimensional approach, combining experimentation and computation, has illuminated the once-enigmatic quark-gluon structure within nucleons. The synergy between theoretical frameworks and empirical observations forms the bedrock of our contribution to particle physics.

Acknowledgments

Our heartfelt thanks go to our dedicated supervisor, Sardar Nabi. His expert insights and unwavering support played a pivotal role in shaping the trajectory of this study.

We acknowledge the contributions of our colleagues and peers for their stimulating discussions and collaborative spirit, which greatly influenced the development of our ideas and methodologies. Additionally, we are grateful to the department of physics, Post Graduate College affiliated with Abdul Wali Khan University Mardan (AWKUM) staff for their assistance in data collection and analysis.

ORCID of Author:

<https://orcid.org/0009-0001-7309-287X> (kamil khan)

corresponding author

<https://orcid.org/0009-0006-9276-4463> (Muhammad Shershah)

<https://orcid.org/0009-0002-0428-7216> (Muhammad Bilal)

<https://orcid.org/0009-0006-8665-2369> (wiqar ahmad)

<https://orcid.org/0009-0007-1070-5599> (Nehad ali)

<https://orcid.org/0009-0001-5156-7010> (Muhammad Arsalan)

<https://orcid.org/0009-0009-9527-2431> (Tauseef Ahmad)

<https://orcid.org/0009-0007-1757-670X> (adnan khan)

<https://orcid.org/0009-0001-0452-0439> (Haider ali khan)

<https://orcid.org/0009-0002-4763-5372> (Sardar nabi)

<https://orcid.org/0009-0001-9250-4198> (jaweria taj)

Conflicts of Interest

The authors declare no conflicts of interest.

References

- [1] A. G.-D. Ridder, T. Gehrmann, E. W. N. Glover, and G. Heinrich, "Jet rates in electron-positron annihilation at $O(\alpha_s^3)$ in QCD," Feb. 2008, doi: 10.1103/PhysRevLett.100.172001.
- [2] (Cern), X. Garcia I Tormo, and; G Luisoni, "Speakers," MPI. [Online]. Available: <http://indico.cern.ch/e/alphas2015>
- [3] K. Khan, A. Hamza, L. Ali, and S. Nabi, "Solar Wind interaction with the Atmosphere of Mars," *Saudi J. Eng. Technol.*, vol. 8, no. 11, pp. 274–282, Nov. 2023, doi: 10.36348/sjet.2023.v08i11.002.
- [4] Nabia, S., & Khanb, J. Solar Wind Interaction with Venus Atmosphere.
- [5] S. Dulat *et al.*, "New parton distribution functions from a global analysis of quantum chromodynamics," *Phys. Rev. D*, vol. 93, no. 3, p. 033006, Feb. 2016, doi: 10.1103/PhysRevD.93.033006.
- [6] Tevatron Electroweak Working Group, "Combination of CDF and D0 results on the W boson mass and width," Aug. 2008.
- [7] K. S. Lee, J. L. Collins, M. J. Anzivino, E. A. Frankel, and F. Schottler, "Heterotopic neurogenesis in a rat with cortical heterotopia," *J. Neurosci.*, vol. 18, no. 22, pp. 9365–75, Nov. 1998, doi: 10.1523/JNEUROSCI.18-22-09365.1998.
- [8] J. McGowan, T. Cridge, L. A. Harland-Lang, and R. S. Thorne, "Approximate N^3 LO Parton Distribution Functions with Theoretical Uncertainties: MSHT20a N^3 LO PDFs," Jul. 2022, doi: 10.1140/epjc/s10052-023-11236-0.
- [9] S. Weinzierl, "NNLO corrections to 3-jet observables in electron-positron annihilation," Jul. 2008, doi: 10.1103/PhysRevLett.101.162001.
- [10] M. Davier, A. Hoecker, B. Malaescu, and Z. Zhang, "Reevaluation of the Hadronic Contributions to the Muon $g-2$ and to $\alpha(MZ)$," Oct. 2010, doi: 10.1140/epjc/s10052-010-1515-z.
- [11] J. F. Owens and W. Tung, "Parton Distribution Functions of Hadrons," *Annu. Rev. Nucl. Part. Sci.*, vol. 42, no. 1, pp. 291–332, Dec. 1992, doi: 10.1146/annurev.ns.42.120192.001451.
- [12] G. Dissertori *et al.*, "Determination of the strong coupling constant using matched NNLO+NLLA predictions for hadronic event shapes in e^+e^- annihilations," Jun. 2009, doi: 10.1088/1126-6708/2009/08/036.